A Particle Filtering Approach for Joint Detection/Estimation of Multipath Effects on GPS Measurements

Audrey Giremus, Jean-Yves Tourneret, and Vincent Calmettes

***Abstract*—Multipath propagation causes major impairments to global positioning system (GPS) based navigation. Multipath results in biased GPS measurements, hence inaccurate position estimates. In this paper, multipath effects are considered as abrupt changes affecting the navigation system. A multiple model formulation is proposed whereby the changes are represented by a discrete valued process. The detection of the errors induced by multipath is handled by a Rao-Blackwellized particle filter (RBPF). The RBPF estimates the indicator process jointly with the navigation states and multipath biases. The interest of this approach is its ability to integrate *a priori* constraints about the propagation environment. The detection is improved by using information from near future GPS measurements at the particle filter (PF) sampling step. A computationally modest delayed sampling is developed, which is based on a minimal duration assumption for multipath effects. Finally, the standard PF resampling stage is modified to include an hypothesis test based decision step.**

***Index Terms*—Delayed sampling, GPS navigation, multipath, multiple models, particle filtering.**

I. INTRODUCTION

RECURSIVE estimation is of primary interest for navigation and tracking problems. The issue is to compute the kinematic state (the position and its derivative) of moving vehicles from noisy measurements from a cluster of sensors. It may be crucial that the estimation is performed on line, for instance to ensure flight safety for an aircraft. The Kalman filter, introduced in [1] and further studied in many textbooks such as [2], has been applied to a wide range of practical problems. This popular algorithm is optimal (in the sense that it minimizes the mean square estimation error) only in the case of linear Gaussian systems. Local linearization schemes yield computationally modest suboptimal solutions for a wide range of nonlinear systems. However, these approximations fail in case of severe nonlinearities. Particle filters (PFs) are promising alternatives in such cases. They have recently received a renewed interest, see for instance [3] or [4] for an overview on the subject. PFs combine importance sampling and resampling steps to generate Monte Carlo approximations of the *posterior* probability density functions (pdfs) of interest. Thus, they can cope with non standard state space models which exhibit non-Gaussian *priors* and/or highly nonlinear equations.

In many practical situations, the studied systems experience nonlinear phenomena such as abrupt changes. These changes can result for instance from a sensor failure or an unexpected maneuver of the vehicle in tracking applications. They can considerably degrade the estimation solution, which explains the active research conducted for change detection. A nearly exhaustive overview of abrupt change algorithms can be for instance found in [5]. Mean jumps in linear systems have also been extensively studied in [6] where likelihood ratio based methods such as the well-known generalized likelihood ratio (GLR) and the CUSUM algorithm are proposed. Other solutions are provided by multiple model formulation. This approach assumes the unknown states obey competing models whose parameters depend on a latent process indicating the possible changes. In this way, *a priori* information about the frequency and amplitude of the changes can be directly appended to the state model. Hence, the detection is made easier. The most popular algorithms, including the Interacting Multiple Models (IMM) or the Generalized Pseudo-Bayes (GPB), are thoroughly described in [7]. Due to their applicability to any class of state space model, PFs also offer a convenient solution to multiple model problems. Efficient algorithms have been developed for that purpose in [8] and [9].

This paper deals with GPS navigation, i.e., a vehicle estimating its own motion from received satellite signals. More precisely, an improved PF is proposed to tackle the problem of multipath which can severely degrade the GPS measurements and thereby the positioning solution. A Rao-Blackwellized technique is applied so that multipath effects detection is handled by a PF technique while both navigation states and multipath errors are estimated by a bank of conditional extended Kalman filters (EKFs). The PF efficiency is known to be greatly improved by using near future measurements at the sampling step [10]. The so-called delayed sampling approach has for instance been developed for adaptive detection and decoding in flat-fading channels in [11]. In this paper, delayed sampling is used to generate relevant samples for multipath detection. A computationally cheaper procedure is developed that takes advantage of the

Manuscript received September 21, 2005; revised May 5, 2006. This paper was presented in part at the International Conference on Acoustics, Speech, and Signal Processing, Philadelphia, PA,March 2005. The associate editor coordinating the review of this paper and approving it for publication was Prof. Simon J. Godsill.

A. Giremus is with SUPAÉRO/TESA, Camichel, BP 7122, 31071 Toulouse Cedex, France, and also with the Enac-Département EL/X 7, BP 54005-31055 Toulouse Cedex 4, France (e-mail: audrey.giremus@enseeiht.fr; giremus@recherche.enac.fr).

J.-Y. Tourneret is with the IRIT/ENSEEIHT/TESA, BP 7122, 31071 Toulouse Cedex, France, and also with the IRIT-ENSEEIHT-TéSA, BP 7122, 31071 Toulouse Cedex 7, France (e-mail: j-y.tourneret@ieee.org; Jean-Yves.tourneret@enseeiht.fr).

V. Calmettes is with the SUPAÉRO, 31055 Toulouse Cedex 4, France (e-mail: vincent.calmettes@supaero.fr).

Digital Object Identifier 10.1109/TSP.2006.888895

sparseness of multipath events. The proposed algorithm also includes an hypothesis test-aided resampling step. Whenever a multipath event is detected, all the particles refuting this hypothesis are penalized to speed up their removal. Thus, the estimation of the incoming states is improved and no computational cost is devoted to update irrelevant samples. The resulting algorithm compares favorably with standard multiple model approaches and provides better multipath bias estimates than the GLR algorithm.

The paper is organized as follows. The problem of GPS navigation in the presence of multipath is described in Section II. Section III introduces a multiple model formulation of this problem. Section IV proposes a fixed-lag Rao-Blackwellized partical filter (RBPF) to solve the joint detection/estimation of multipath effects on the GPS measurements. Simulation results and conclusions are reported in Sections V and VI.

II. Background

The global positioning system (GPS) is extensively used as a navigation system due to its world-wide coverage, low cost, and accuracy. GPS allows any vehicle equipped with a receiver to compute its position, velocity, and so forth. GPS receivers measure time delays of signals from in-view satellites, hence range measurements. These measurements are biased due to receiver and satellite clock offsets. Thus, they are denoted as pseudoranges. Four simultaneous measurements are necessary to solve the so-called navigation problem: estimate the vehicle position in three-dimension and the GPS clock offset.

Multipath propagation highly degrades GPS tracking performance. Multipath occurs when the satellite signal is reflected on different surfaces (ground, block of buildings) before arriving to the receiver. Therefore, the incoming signal is the sum of the direct signal and several delayed replica. Usual GPS receivers, based on the single-path assumption, estimate a wrong propagation delay. A closer look over GPS receiver techniques allows us to plainly understand multipath effects. The transmitted GPS signals are spread using pseudorandom noise (PRN) sequences whose correlation peak is very sharp. They are correlated in the receiver by a local shifted replica of the PRN code until maximal correlation occurs. The local signal phase then provides the incoming signal time of arrival. However, the correlation peak is distorted in the presence of one or more reflected components, yielding biased pseudoranges [12]. Note that multipath errors are bounded since signals with delays larger than a code chip are uncorrelated with the direct signal. Simulations carried out in [13] show that multipath can result in biases of up to 100 m. Consequently, multipath appears as a critical issue.

There has been a surge of interest for mitigation techniques in the past few years. The proposed solutions are aimed either to recover the unbiased propagation delay or to compensate for the induced errors on GPS measurements. A wide range of techniques has been proposed in the first case. Some of these techniques require to modify the receiver architecture. In [14] and [15], a narrow correlator proves efficient to reduce the bias. Other approaches jointly estimate the direct and reflected signal parameters, either directly from the received signal [16] or by means of an EKF based delay lock loop [17]. This study focuses on the second class of methods which track multipath biases on the GPS pseudoranges. A straightforward approach consists of estimating jointly the navigation states and the multipath biases from the corrupted GPS measurements. The tracking can be carried out by an EKF as advocated by [18] for wireless positioning systems. Such an algorithm has been shown to significantly improve positioning accuracy in a known multipath environment. Its main limitation is that multipath biases are estimated even in the absence of multipaths. The *a priori* dynamics of biases cannot be adjusted to cope at the same time with the abrupt jumps and the nearly constant periods. As an alternative, this paper presents a joint detection/estimation technique. Thus, the state space model is modified to include multipath biases only if a bias is detected on the GPS measurements.

III. Problem Formulation

This paper proposes to handle multipath effects by a joint detection/estimation strategy based on a multiple model formulation. Multipath appearance or disappearance result in a mean value jump in the measurement equation, hence, an abrupt change in the state space model. The classical navigation model is extended in this paper by including both the multipath biases and a latent process $\{\boldsymbol{\lambda}_t\}_{t>0}$ which represents multipath occurrences

$$\begin{pmatrix} \boldsymbol{x}_t \\ \boldsymbol{m}_t \end{pmatrix} = F_t \begin{pmatrix} \boldsymbol{x}_{t-1} \\ \boldsymbol{m}_{t-1} \end{pmatrix} + \boldsymbol{v}_t \quad (1)$$

$$\boldsymbol{Y}_t = g_t(\boldsymbol{x}_t) + C(\boldsymbol{\lambda}_{0:t})\boldsymbol{m}_t + \boldsymbol{w}_t \quad (2)$$

where

- $\boldsymbol{v}_t \sim \mathcal{N}(\boldsymbol{0}, Q_t)$ and $\boldsymbol{w}_t \sim \mathcal{N}(\boldsymbol{0}, R_t)$ are independent Gaussian white noise sequences (the notation $\mathcal{N}(\boldsymbol{m}, P)$ refers to a Gaussian distribution of mean $\boldsymbol{m}$ and covariance matrix P);
- $\boldsymbol{x}_t \in \mathbb{R}^{n_x}$ is the navigation vector, composed of the four unknowns (the vehicle position and the GPS receiver clock offset) and their derivatives;
- $\boldsymbol{Y}_t \in \mathbb{R}^{n_y}$ is the measurement vector, formed of the GPS pseudoranges at time t. The dimension n_y coincides with the number of in-view GPS satellites;
- $\boldsymbol{m}_t \in \mathbb{R}^{n_y}$ is the vector of multipath biases (each component is associated with one of the GPS measurement);
- $\boldsymbol{\lambda}_t \in \mathbb{R}^{n_y}$ indicates the possible mean value jumps on the GPS measurements at time t. The vector $\boldsymbol{\lambda}_t$ takes its values in a finite set $\Lambda = \{0,1\}^{n_y}$, such that $\boldsymbol{\lambda}_{t,i} = 1$ if a multipath bias appears on the ith GPS measurement and $\boldsymbol{\lambda}_{t,i} = 0$ otherwise. Λ is formed of $2^{n_y} = n_\Lambda$ elements denoted $\{\boldsymbol{\lambda}^j\}_{j=1,\ldots,n_\Lambda}$. Note that, in this paper, the classical notation $\boldsymbol{\lambda}_{0:t} = (\boldsymbol{\lambda}_0, \ldots, \boldsymbol{\lambda}_t)$ is used.

Denote as $\boldsymbol{X}_t = (\boldsymbol{x}_t^T, \boldsymbol{m}_t^T)^T$ the vector containing the unknown continuous valued parameters. The state and measurement models related to $\boldsymbol{X}_t$ and $\boldsymbol{\lambda}_t$ are detailed.

A. State Model

1) Navigation States/Multipath Biases: Classical dynamic models can be used in navigation depending on the dynamic level of the vehicle. The reader is invited to read [9] for an overview on this subject. In this paper, the vehicle is assumed to be in uniform motion (i.e., near constant velocity). Therefore, a second-order model fully characterizes its dynamic behavior. The state vector then only includes the following parameters:

$$\boldsymbol{X}_t = \left(x_t, \dot{x}_t, y_t, \dot{y}_t, z_t, \dot{z}_t, b_t, \dot{b}_t, \boldsymbol{m}_t^T, \dot{\boldsymbol{m}}_t^T\right)^T$$

where

- (x_t, y_t, z_t) is the vehicle position in the Earth centered Earth fixed frame (ECEF), denoted $\boldsymbol{p}_t$;
- $(\dot{x}_t, \dot{y}_t, \dot{z}_t)$ is the vehicle velocity;
- $(b_t, \dot{b}_t)$ are the GPS clock offset and clock drift, respectively;
- $\boldsymbol{m}_t$ and $\dot{\boldsymbol{m}}_t$ comprise the multipath biases and their derivatives, respectively.

The velocity is reasonably modeled as a random walk process (of variance σ_a^2) and the position is obtained by integration. The GPS clock drift is usually represented as a Gauss Markov process which is integrated to yield the GPS clock offset [19]. Such a model is reasonable for short-term applications as it does not take into account the periodical clock resets performed by the GPS receiver. The multipath biases can be well modeled as random walks (of variance σ_m^2). The overall state matrices are block-diagonal due to the relative independence of the kinematic parameters, the GPS clock parameters and the multipath biases. They can be defined as follows:

$$F_t = \begin{pmatrix} A_t & \mathbf{0} & \mathbf{0} \\ \mathbf{0} & C_t & \mathbf{0} \\ \mathbf{0} & \mathbf{0} & \mathrm{I} \end{pmatrix} \quad \text{and} \quad Q_t = \begin{pmatrix} \Sigma_t^a & \mathbf{0} & \mathbf{0} \\ \mathbf{0} & \Sigma_t^c & \mathbf{0} \\ \mathbf{0} & \mathbf{0} & \sigma_m^2 \mathrm{I} \end{pmatrix}$$

where the block matrices A_t, C_t, Σ_t^a, and Σ_t^c have the following form:

$$A_t = \begin{pmatrix} C_t & \mathbf{0} & \mathbf{0} \\ \mathbf{0} & C_t & \mathbf{0} \\ \mathbf{0} & \mathbf{0} & C_t \end{pmatrix}, \quad \text{with} \quad C_t = \begin{pmatrix} 1 & \Delta t \\ 0 & 1 \end{pmatrix}$$

$$\Sigma_t^a = \begin{pmatrix} Q_t^a & \mathbf{0} & \mathbf{0} \\ \mathbf{0} & Q_t^a & \mathbf{0} \\ \mathbf{0} & \mathbf{0} & Q_t^a \end{pmatrix}, \quad \text{with}$$

$$Q_t^a = \begin{pmatrix} \sigma_a^2 \frac{\Delta t^3}{3} & \sigma_a^2 \frac{\Delta t^2}{2} \\ \sigma_a^2 \frac{\Delta t^2}{2} & \sigma_a^2 \Delta t \end{pmatrix}$$

$$\Sigma_t^c = \begin{pmatrix} \sigma_b^2 \Delta t + \sigma_d^2 \frac{\Delta t^3}{3} & \sigma_d^2 \frac{\Delta t^2}{2} \\ \sigma_d^2 \frac{\Delta t^2}{2} & \sigma_d^2 \Delta t \end{pmatrix}.$$

The variances σ_a^2 and σ_m^2 depend on the application (driving in a urban environment, air-flight ...), whereas the corresponding values for the GPS clock parameters σ_b^2 and σ_d^2 have been extensively studied and are inventoried in tables [9]. The sampling period has been denoted Δt in the previous expressions.

2) Indicator Process: The process $\boldsymbol{\lambda}_t$ takes on scattered nonzero values. Each component can be modeled as a Bernoulli random variable:

$$P[\boldsymbol{\lambda}_{t,i} = 1] = \gamma \text{ and } P[\boldsymbol{\lambda}_{t,i} = 0] = 1 - \gamma.$$

The parameter γ depends on the propagation environment. For instance, rural areas are characterized by very low values of γ whereas urban areas require higher values of γ.

B. Measurement Model

At each time instant, the measurement vector is composed of the pseudoranges associated with in-view GPS satellites. The nonlinear function g_t, appearing in (2), is the mathematical expression for the distances between the vehicle and the GPS satellites which are corrupted by the additive GPS receiver clock offset. Depending on the propagation environment, any measurement can be affected by multipath at a given time instant t. An additional process $\boldsymbol{\epsilon}_t$ is introduced to represent the presence/absence of multipath biases on the measurements. It is related to the change indicator as follows:

$$\boldsymbol{\epsilon}_{t,i} = \boldsymbol{\epsilon}_{t-1,i} \quad \text{if } \boldsymbol{\lambda}_{t,i} = 0$$
$$\boldsymbol{\epsilon}_{t,i} = 1 - \boldsymbol{\epsilon}_{t-1,i} \quad \text{if } \boldsymbol{\lambda}_{t,i} = 1.$$

Note that the component $\boldsymbol{\epsilon}_{t,i}$ is equal to $\oplus_{k=1}^{t} \boldsymbol{\lambda}_{k,i}$ (where $\oplus$ is the exclusive or), with $\boldsymbol{\epsilon}_{0,i} = \mathbf{0}$ (assuming no multipath at time $t = 0$).

The corresponding measurement equation can finally be expressed as

$$\boldsymbol{Y}_{t,i} = \left\| \boldsymbol{s}_t^i - \boldsymbol{p}_t \right\| + b_t + \boldsymbol{\epsilon}_{t,i} \boldsymbol{m}_{t,i} + \boldsymbol{w}_{t,i}$$

where

- $\boldsymbol{Y}_{t,i}$ is the ith component of the measurement vector ($i = 1, \ldots, n_y$), or equivalently the GPS pseudorange associated with the ith GPS satellite;
- $\boldsymbol{s}_t^i$ is the ith GPS satellite position;
- the covariance matrix of the measurement noise $\boldsymbol{w}_t$ satisfies $R_t = \sigma^2 \mathrm{I}$, with σ the standard GPS ranging error.

The previous model includes both continuous and discrete valued processes. Moreover, the GPS measurements are nonlinearly related to the unknown state vector. Consequently, sequential Monte Carlo methods offer an appropriate framework for the estimation of the mixed state vector $(\boldsymbol{X}_t, \boldsymbol{\lambda}_t)$.

IV. A Particle Filtering Approach

In a Bayesian framework, all inference about the unknown parameters is based on their *posterior* distribution. The joint detection/estimation of multipath effects on GPS measurements is handled by estimating the *posterior* pdf of the augmented state vector $(\boldsymbol{X}_{0:t}, \boldsymbol{\lambda}_{0:t})$ conditioned on the measurements up to the current time, denoted as $p(\boldsymbol{X}_{0:t}, \boldsymbol{\lambda}_{0:t} | \boldsymbol{Y}_{1:t})$. A recursive application of Bayes' rule allows to derive a conceptual solution to the estimation problem. The indicator process can be marginalized out to yield the posterior pdf of the navigation states and multipath biases:

$$p(\boldsymbol{X}_t | \boldsymbol{Y}_{1:t}) = \sum_{i=1}^{n_\Lambda^t} \omega_t^{(i)} p\left(\boldsymbol{X}_t \middle| \boldsymbol{Y}_{1:t}, \boldsymbol{\lambda}_{0:t}^{(i)}\right) \tag{3}$$

where

$$\omega_t^{(i)} = P\left[\boldsymbol{\lambda}_{0:t}^{(i)} \middle| \boldsymbol{Y}_{1:t}\right] \tag{4}$$

$$\omega_t^{(i)} \propto \prod_{k=1}^{t} p\left(\boldsymbol{Y}_k \middle| \boldsymbol{\lambda}_{0:k}^{(i)}, \boldsymbol{Y}_{1:k-1}\right) P\left[\boldsymbol{\lambda}_k^{(i)}\right]. \tag{5}$$

The pdfs $p(\boldsymbol{X}_t|\boldsymbol{Y}_{1:t},\boldsymbol{\lambda}_{0:t}^{(i)})_{t>0}$ and $p(\boldsymbol{Y}_k|\boldsymbol{\lambda}_{0:k}^{(i)},\boldsymbol{Y}_{1:k-1})_{k=1:t}$ can be estimated by parallel EKFs, provided the measurement model nonlinearities are small enough as shown in [20]. However, the sum in (3) covers an exponentially growing number of discrete sequences $\boldsymbol{\lambda}_{0:t}$. A selection procedure needs to be applied to keep the computational complexity constant. Several algorithms have been developed in the literature, which are based either on a pruning or a merging strategy (see [7] for an overview on the subject). The most popular algorithms include the IMM and the GPB. SMC methods also offer a convenient and flexible framework to handle such problems. The main difference is that the possible hypotheses are not explored exhaustively but randomly according to a simulation-based rule. Indeed, PFs automatically focuses on the most likely paths $\boldsymbol{\lambda}_{0:t}$ according to a combination of sampling/resampling steps. This section shows that the GPS navigation problem defined by (1) and (2) can be advantageously solved by a Rao-Blackwellized technique, where only the discrete valued process distribution is approximated by a PF approach.

A. RBPFs

Many strategies can be implemented to improve PF efficiency. Rao-Blackwellization is a well-known technique to decrease the variance of the state estimates for conditionally linear Gaussian state space models. The principle is to solve analytically the conditional linear part while the nonlinear part is estimated by a PF method. This approach has received much interest in the literature, see for instance [21]–[23] or [24]. In our application, the state space model is "almost linear" Gaussian conditioned on the indicator sequence $\boldsymbol{\lambda}_{0:t}$ ("Almost linear" means that the nonlinearities can be handled by local linearizations without introducing too much inaccuracy). The validity of this assertion has been discussed for instance in [20], wherein the estimation error of an EKF is shown to meet the posterior Cramer Rao bound for a GPS positioning problem. The RB technique is based on the following factorization of the unknown pdf of interest:

$$p(\boldsymbol{X}_t,\boldsymbol{\lambda}_{0:t}|\boldsymbol{Y}_{1:t}) = p(\boldsymbol{X}_t|\boldsymbol{\lambda}_{0:t},\boldsymbol{Y}_{1:t})P[\boldsymbol{\lambda}_{0:t}|\boldsymbol{Y}_{1:t}].$$

The conditional *posterior* pdfs $p(\boldsymbol{X}_t|\boldsymbol{\lambda}_{0:t},\boldsymbol{Y}_{1:t})$ can then be estimated by Gaussian distributions whose first- and second-order moments are computed by standard recursions of EKFs. Consequently, only the discrete valued process $\boldsymbol{\lambda}_t$ is estimated by a PF technique. Of course, the state vector $\boldsymbol{X}_t$ could be also estimated by a PF technique. However, this strategy has not been considered here since it would require to use more particles to obtain a slightly better estimation performance. The different steps allowing to estimate the state vector $\boldsymbol{X}_t$ and the indicator sequence $\boldsymbol{\lambda}_{0:t}$ are detailed in what follows.

1) Estimation of $\boldsymbol{\lambda}_{0:t}$*:* PFs provide a point mass approximation of the distribution of interest:

$$\hat{P}[\boldsymbol{\lambda}_{0:t}|\boldsymbol{Y}_{1:t}] = \sum_{i=1}^{N}\omega_t^{(i)}\delta\left(\boldsymbol{\lambda}_{0:t}-\boldsymbol{\lambda}_{0:t}^{(i)}\right) \tag{6}$$

where δ denotes the Dirac distribution. The support points $\boldsymbol{\lambda}_{0:t}^{(i)}$ are called particles, and the elementary probabilities $\omega_t^{(i)}$ importance weights. This empirical estimation is obtained from a combination of importance sampling/resampling steps. In a few words, it is usually impossible to simulate the particles directly from the target distribution P. As an alternative, they are drawn sequentially from a proposal distribution Π

$$\boldsymbol{\lambda}_t \sim \Pi\left(\boldsymbol{\lambda}_t\,\middle|\,\boldsymbol{\lambda}_{0:t-1}^{(i)},\boldsymbol{Y}_{1:t}\right).$$

The particles are assigned weights according to their relevance with regard to P. PFs also include a resampling step which consists of generating a new set of particles according to the estimated discrete distribution. Thus, PF degeneracy is avoided by selecting relevant particles. A comprehensive presentation of these methods and their applications is found in [3].

2) Estimation of $\boldsymbol{X}_{0:t}$*:* Each particle $\boldsymbol{\lambda}_{0:t}^{(i)}$ is associated with a conditional EKF that computes recursively

$$\begin{aligned}
\hat{p}\left(\boldsymbol{X}_t\,\middle|\,\boldsymbol{\lambda}_{0:t}^{(i)},\boldsymbol{Y}_{1:t}\right) &= \mathcal{N}\left(\hat{\boldsymbol{X}}_t^{(i)},P_t^{(i)}\right)\\
\hat{p}\left(\boldsymbol{Y}_t\,\middle|\,\boldsymbol{\lambda}_{0:t}^{(i)},\boldsymbol{Y}_{1:t-1}\right) &= \mathcal{N}\left(\hat{\boldsymbol{Y}}_t^{(i)},S_t^{(i)}\right)\\
\hat{p}\left(\boldsymbol{X}_t\,\middle|\,\boldsymbol{\lambda}_{0:t}^{(i)},\boldsymbol{Y}_{1:t-1}\right) &= \mathcal{N}\left(\hat{\boldsymbol{X}}_{t|t-1}^{(i)},P_{t|t-1}^{(i)}\right).
\end{aligned}$$

It results that the marginal distributions of the continuous valued states are estimated by mixtures of Gaussian distributions

$$\hat{p}(\boldsymbol{X}_t|\boldsymbol{Y}_{1:t}) = \sum_{i=1}^{N}\omega_t^{(i)}\hat{p}\left(\boldsymbol{X}_t\,\middle|\,\boldsymbol{\lambda}_{0:t}^{(i)},\boldsymbol{Y}_{1:t}\right).$$

Note that RBPFs are very similar to classical multiple model algorithms. Indeed, the estimation is performed from a bank of conditional EKFs, each corresponding to a possible indicator path $\boldsymbol{\lambda}_{0:t}^{(i)}$ or equivalently to a possible multipath scenario. The main difference between these approaches lies in the way the indicator paths are explored. The possible hypotheses are not investigated exhaustively with RBPFs, contrary to usual multiple model algorithms. Indeed, the simulation step allows to propose directly interesting candidates.

This paper proposes some improvements to the classical RBPF to satisfy the detection/estimation objectives: an approximate delayed sampling technique, a fixed lag smoothing estimation and a decision-aided resampling, resulting in the so-called fixed-lag RBPF.

B. The Fixed Lag RBPF

1) Approximate Delayed Sampling: Multipath occurrences result in a temporary mean value jump affecting GPS measurements. Consequently, near future measurements reveal useful information about the indicator state at the current time $\boldsymbol{\lambda}_t$. The proposed algorithm makes use of future observations to generate the current particles as suggested in [11]. This procedure is called delayed sampling. Such a method turns out to be beneficial and possibly even crucial depending on the propagation environment (urban or rural areas):

- multipath appearance/disappearance are sparse events, hence the probability γ can be very low. If the particles were only simulated according to their *prior* distribution, the number of samples indicating a mean value jump would be negligible;

- depending on their amplitudes, the induced mean value jumps can be embedded in the measurement noise. Hence, several observations are required to detect multipath occurrence;
- delayed sampling prevents false detections and, thus, makes the algorithm more robust to outliers.

Information from near future measurements is included by simulating from the fixed lag smoothing distribution $P[\boldsymbol{\lambda}_t|\boldsymbol{\lambda}_{0:t-1}^{(i)}, \boldsymbol{Y}_{1:t+L}]$ (for $i = 1, \ldots, N$), where L is a positive integer corresponding to the length of the observation window. Proposals of this form significantly increase the number of particles indicating a mean jump when multipath occurs. The indicator vector $\boldsymbol{\lambda}_t$ takes value in a finite set of cardinal n_Λ. Therefore, all the possible future paths can be explored to compute the proposal distribution as

$$P[\boldsymbol{\lambda}_t|\boldsymbol{\lambda}_{0:t-1}, \boldsymbol{Y}_{1:t+L}] = \sum_{\boldsymbol{\lambda}_{t+1:t+L}} P[\boldsymbol{\lambda}_t, \boldsymbol{\lambda}_{t+1:t+L}|\boldsymbol{\lambda}_{0:t-1}, \boldsymbol{Y}_{1:t+L}].$$

However, the computational complexity is prohibitive since the sum covers a growing number of values with the lag. In [11], a low-complexity technique based on a random exploration of the future states is presented. This paper proposes a simpler procedure where only the *a priori* most probable future paths are considered. An absence of jump during the observation window (from time $t+1$ to $t+L$) is *a priori* far more likely than any other hypothesis due to the sparseness of multipath events. Thus, the fixed lag smoothing proposal distribution is approximated as

$$P\left[\boldsymbol{\lambda}_t \left|\boldsymbol{\lambda}_{0:t-1}^{(i)}, \boldsymbol{Y}_{1:t+L}\right.\right] \simeq P\left[\boldsymbol{\lambda}_t, \boldsymbol{\lambda}_{t+1:t+L} = \mathbf{0}\left|\boldsymbol{\lambda}_{0:t-1}^{(i)}, \boldsymbol{Y}_{1:t+L}\right.\right].$$

The resulting distribution, referred to as approximate delayed sampling proposal, takes the form

$$P\left[\boldsymbol{\lambda}_t \left|\boldsymbol{\lambda}_{0:t-1}^{(i)}, \boldsymbol{Y}_{1:t+L}\right.\right] \simeq \sum_{j=1}^{n_\lambda} \gamma^{(i,j)} \delta(\boldsymbol{\lambda}_t - \boldsymbol{\lambda}^j)$$

where $\gamma^{(i,j)} \propto P[\boldsymbol{\lambda}_t = \boldsymbol{\lambda}^j, \boldsymbol{\lambda}_{t+1:t+L} = \mathbf{0}|\boldsymbol{\lambda}_{0:t-1}^{(i)}, \boldsymbol{Y}_{1:t+L}]$.

Introduce the following notation before detailing the computations leading to the probabilities $\gamma^{(i,j)}$:

$$\left(\boldsymbol{\Lambda}_{t-l}^{t+k}\right)^{(i,j)} = \left(\boldsymbol{\lambda}_{t-l:t-1}^{(i)}, \boldsymbol{\lambda}_t = \boldsymbol{\lambda}^j, \boldsymbol{\lambda}_{t+1:t+k} = \mathbf{0}\right).$$

The probabilities $\gamma^{(i,j)}$ can be expressed as follows:

$$\gamma^{(i,j)} = \tilde{\gamma}^{(i,j)} \Bigg/ \left(\sum_{k=1}^{n_\Lambda} \tilde{\gamma}^{(i,k)}\right)$$

where

$$\tilde{\gamma}^{(i,j)} \propto \left(\prod_{k=0}^{L} p\left(\boldsymbol{Y}_{t+k}\left|\boldsymbol{Y}_{1:t+k-1}, \left(\boldsymbol{\Lambda}_0^{t+k}\right)^{(i,j)}\right.\right)\right) \times P[\boldsymbol{\lambda}_t = \boldsymbol{\lambda}^j] \quad (7)$$

In (7), the predictive pdfs $p(\boldsymbol{Y}_{t+k}|\boldsymbol{Y}_{1:t+k-1}, (\boldsymbol{\Lambda}_0^{t+k})^{(i,j)})$ are obtained by running L iterations of the n_Λ EKFs conditional on the considered future paths $((\boldsymbol{\Lambda}_0^{t+k})^{(i,j)})_{j=1,\ldots,n_\Lambda}$.

2) Estimation: The filtering importance weights can be updated classically as the ratio of the target and the proposal distributions. If the index j^i refers to the drawing result for the particle $\boldsymbol{\lambda}_t^{(i)}$ (i.e., $\boldsymbol{\lambda}_t^{(i)} = \boldsymbol{\lambda}^{j^i}$), the weights $\omega_t^{(i)}$ can be classically computed as follows:

$$\omega_t^{(i)} \propto \omega_{t-1}^{(i)} \frac{p\left(\boldsymbol{Y}_t\left|\boldsymbol{Y}_{0:t-1}, \boldsymbol{\lambda}_{0:t}^{(i)}\right.\right) P\left[\boldsymbol{\lambda}^{j^i}\right]}{\gamma^{(i,j^i)}}. \quad (8)$$

However, the delayed sampling rather suggests a fixed-lag smoother PF, whereby tighter estimates are computed from the smoothing distribution $P[\boldsymbol{\lambda}_t|\boldsymbol{Y}_{1:t+L}]$. A theoretically valid smoothing approach would require exploring the entire future state space to generate candidate particles $\boldsymbol{\lambda}_{t:t+L}^{(i)}$. The difficulty is easily overcome by considering the particles $(\boldsymbol{\Lambda}_t^{t+L})^{(i,j^i)}$ as samples from the smoothing proposal $P[\boldsymbol{\lambda}_{t:t+L}|\boldsymbol{Y}_{1:t+L}, \boldsymbol{\lambda}_{0:t-1}^{(i)}]$, as proposed in [11]. Smoothing weights can then be computed as follows:

$$\tilde{\omega}_t^{(i)} \propto \omega_{t-1}^{(i)} p\left[\left(\boldsymbol{\Lambda}_t^{t+L}\right)^{(i,j^i)}\right] \times \frac{\prod_{k=0}^{L} p\left(\boldsymbol{Y}_{t+k}\left|\boldsymbol{Y}_{0:t+k-1}, \left(\boldsymbol{\Lambda}_0^{t+k}\right)^{(i,j^i)}\right.\right)}{\gamma^{(i,j^i)}}$$

which yields

$$\tilde{w}_t^{(i)} \propto \omega_{t-1}^{(i)} \left(\sum_{k=1}^{n_\Lambda} \tilde{\gamma}^{(i,k)}\right). \quad (9)$$

Hence, the empirical approximation of the smoothing distribution can be written as

$$\hat{P}[\boldsymbol{\lambda}_{0:t+L}|\boldsymbol{Y}_{1:t+L}] = \sum_{i=1}^{N} \tilde{\omega}_t^{(i)} \delta\left(\boldsymbol{\lambda}_{0:t+L} - \left(\boldsymbol{\Lambda}_0^{t+L}\right)^{(i,j^i)}\right)$$

and an estimate of the desired marginal distribution is

$$\hat{P}[\boldsymbol{\lambda}_t|\boldsymbol{Y}_{1:t+L}] = \sum_{i=1}^{N} \tilde{\omega}_t^{(i)} \delta\left(\boldsymbol{\lambda}_t - \boldsymbol{\lambda}^{j^i}\right).$$

Fixed-lag smoothing significantly improves the estimation accuracy. The continuous state estimates are obtained by combining the conditional EKF outputs

$$\hat{\boldsymbol{X}}_t = \sum_{i=1}^{N} \tilde{\omega}_t^{(i)} \hat{\boldsymbol{X}}_t^{(i)}. \quad (10)$$

Similarly, the detection can be handled by monitoring the change probability, defined as

$$P_t^c = P[\boldsymbol{\lambda}_t \neq 0|\boldsymbol{Y}_{1:t+L}].$$

The corresponding fixed-lag PF approximation is given by

$$\hat{P}_t^c = \sum_{i=1}^{N} \tilde{\omega}_t^{(i)} \left(1 - \delta\left(\boldsymbol{\lambda}_t^{(i)}\right)\right). \tag{11}$$

The change instants are expected to coincide with the estimated probability peaks. Consequently, ad-hoc thresholds might be chosen to decide the occurrence of a mean value jump. Next, a different detection procedure is proposed which allows to overcome this difficulty.

3) Decision Aided Resampling: Several difficulties may arise when applying the proposed algorithm to real navigation scenarios. First, the parameters of the multipath model are difficult to set. In particular, a too small value of the prior probability that a mean jump occurs turns out to be very penalizing for detecting multipath events. Second, a reasonable number of particles should be simulated to keep the computational cost low. This constraint is the price for a possible on-board implementation of the positioning algorithm. Based on these remarks, multipath bias detection may not be clear-cut. It takes a few iterations until all particles switch to indicate a mean jump that affects GPS measurements. This paper argues that a careful selection of the particles at each time step allows to improve multipath bias tracking even if few samples are used. Classically, irrelevant particles are discarded on their own accord at the PF resampling step. In this case, a more efficient scheme can be considered which consists of introducing an hypothesis test to aid resampling. This section first describes the corresponding test statistic. The subsequent modified resampling procedure is then detailed.

Binary Hypothesis Test: The hypotheses under consideration can be written as follows:

- $H_{0,t}$: no multipath event;
- $H_{1,t}$: occurrence of a mean value jump due to multipath.

According to the Neyman-Pearson lemma, the likelihood ratio is an appropriate test statistic to decide between the competing hypotheses. The delayed measurements are crucial to design efficient proposal distributions. Similarly, they are expected to improve the detection. Consequently, the following decision procedure is proposed:

$$T_t = \frac{p(\boldsymbol{Y}_{t:t+L}|\boldsymbol{Y}_{1:t-1}, H_{1,t}, \boldsymbol{\nu}_t)}{p(\boldsymbol{Y}_{t:t+L}|\boldsymbol{Y}_{1:t-1}, H_{0,t})} \underset{H_{0,t}}{\overset{H_{1,t}}{\lessgtr}} h_t \tag{12}$$

where $\boldsymbol{\nu}_t$ is the mean value jump amplitude, estimated by the PF as

$$\hat{\boldsymbol{\nu}}_t = \hat{\boldsymbol{m}}_t - \hat{\boldsymbol{m}}_{t|t-1}$$
$$\hat{\boldsymbol{m}}_{t|t-1} = \sum_{i=1}^{N} \omega_{t-1}^{(i)} \hat{\boldsymbol{m}}_{t|t-1}^{(i)}.$$

The main difficulty is to choose an appropriate threshold test h_t in (12). Usually, h_t is computed as a function of the false alarm rate, $\alpha = P[\text{decide } H_{1,t}|H_{0,t}]$, by solving

$$\alpha = \int_{h_t}^{\infty} p_{H_{0,t}}(u)\, du \tag{13}$$

where $p_{H_{0,t}}(u)$ is the pdf of T_t under hypothesis $H_{0,t}$. Unfortunately, the integral (13) is intractable because $p_{H_{0,t}}(u)$ has not a simple closed-form expression. Therefore, this paper proposes to use an approximate test statistic $\tilde{T}_t$ which allows us to derive a closed-form expression for the threshold.

First, the hypotheses $H_{1,t}$ and $H_{0,t}$ can be rewritten according to the sparseness assumption:

$$H_{1,t} = \{\boldsymbol{\lambda}_t \neq \mathbf{0}, \boldsymbol{\lambda}_{t+1:t+L} = \mathbf{0}\}$$
$$H_{0,t} = \{\boldsymbol{\lambda}_t = \mathbf{0}, \boldsymbol{\lambda}_{t+1:t+L} = \mathbf{0}\}.$$

The Bayes rule then leads to the following approximated expression for T_t

$$T_t \simeq \prod_{k=0}^{L} \frac{p\left(\boldsymbol{Y}_{t+k}|\boldsymbol{Y}_{1:t+k-1}, H_{1,t}, \hat{\boldsymbol{\nu}}_t\right)}{p(\boldsymbol{Y}_{t+k}|\boldsymbol{Y}_{1:t+k-1}, H_{0,t})}. \tag{14}$$

Each likelihood appearing in the ratio (14) can be approximated by a mixture of Gaussian resulting from the RBPF. Under the null hypothesis, the following result can be obtained:

$$p(\boldsymbol{Y}_{t+k}|\boldsymbol{Y}_{1:t+k-1}, H_{0,t}) \simeq \sum_{i=1}^{N} \beta_{t+k}^{(i)} p\left(\boldsymbol{Y}_{t+k} \,\middle|\, \boldsymbol{Y}_{1:t+k-1}, \boldsymbol{\lambda}_{0:t-1}^{(i)}, H_{0,t}\right)$$

where $k = 0, \ldots, L$ and the expression of the weights $\beta_{t+k}^{(i)}$ is detailed in Appendix. The parameters of the conditional distributions $p(\boldsymbol{Y}_{t+k}|\boldsymbol{Y}_{1:t+k-1}, \boldsymbol{\lambda}_{0:t-1}^{(i)}, H_{0,t})$ are computed by the EKFs associated to the particles $\boldsymbol{\lambda}_{0:t+k} = (\boldsymbol{\lambda}_{0:t-1}^{(i)}, \boldsymbol{\lambda}_{t:t+k} = \mathbf{0})$. A solution to obtain a simpler expression for T_t is to merge the Gaussian distributions in a single one by matching the first and second moments

$$p(\boldsymbol{Y}_{t+k}|\boldsymbol{Y}_{1:t+k-1}, H_{0,t}) \simeq \mathcal{N}(\hat{\boldsymbol{Y}}_{t+k}, \hat{S}_{t+k})$$

with

$$\hat{\boldsymbol{Y}}_{t+k} = \sum_{i=1}^{N} \beta_{t+k}^{(i)} \hat{\boldsymbol{Y}}_{t+k}^{(i)}$$
$$\hat{S}_{t+k} = \sum_{i=1}^{N} \beta_{t+k}^{(i)} \left(\hat{S}_{t+k}^{(i)} + \boldsymbol{\varepsilon}_{t+k}^{(i)} \boldsymbol{\varepsilon}_{t+k}^{(i)\,T}\right)$$

with $\boldsymbol{\varepsilon}_{t+k}^{(i)} = \boldsymbol{Y}_{t+k} - \hat{\boldsymbol{Y}}_{t+k}^{(i)}$. Note that this approximation underlies the well-known IMM algorithm [7]. In our application, it makes sense since the decision-aided resampling step automatically switches to the dominating mode of the multimodal estimated pdfs at each time instant. The merging strategy leads to an appealing expression for the test statistic T_t and the threshold h_t. The corresponding calculations are developed hereafter. Let us introduce the innovations in (14) as

$$T_t \simeq \prod_{k=0}^{L} \frac{p(\boldsymbol{\varepsilon}_{t+k}|H_{1,t}, \hat{\boldsymbol{\nu}}_t)}{p(\boldsymbol{\varepsilon}_{t+k}|H_{0,t})}$$

where

$$\boldsymbol{\varepsilon}_{t+k} = \boldsymbol{Y}_{t+k} - \hat{\boldsymbol{Y}}_{t+k} \tag{15}$$

$$= \sum_{i=1}^{N} \beta_{t+k}^{(i)} \varepsilon_{t+k}^{(i)}. \quad (16)$$

In the linear Gaussian case, Willsky has shown in his seminal paper introducing the GLR [25] that the impact of an additive change on the innovations could be made explicit. Therefore, each conditional innovation $\varepsilon_{t+k}^{(i)}$ satisfies

$$\varepsilon_{t+k}^{(i)}[t] = \varepsilon_{t+k}^{(i)} + \left(\varphi_{t+k}^{T}\right)^{(i)} \hat{\nu}_t \quad (17)$$

where $[t]$ refers to the value of the parameter if a mean jump has occurred at time t. The necessary formula to compute the matrices $(\varphi_{t+k}^{T})^{(i)}$ are recalled for instance in [5]. The merged innovations under hypotheses $H_{1,t}$ and $H_{0,t}$ are related the same way

$$\varepsilon_{t+k}[t] = \varepsilon_{t+k} + \varphi_{t+k}^{T} \hat{\nu}_t \quad (18)$$

$$\varphi_{t+k}^{T} = \sum_{i=1}^{N} \beta_{t+k}^{(i)} \left(\varphi_{t+k}^{T}\right)^{(i)}. \quad (19)$$

Thus, their pdfs only differ by their means

$$p(\varepsilon_{t+k}|H_{0,t}) \simeq \mathcal{N}(\mathbf{0}; S_{t+k})$$
$$p(\varepsilon_{t+k}|H_{1,t}, \hat{\nu}_t) \simeq \mathcal{N}\left(\varphi_{t+k}^{T}\hat{\nu}_t; S_{t+k}\right).$$

The approximated test statistic satisfies

$$2 \ln T_t = \sum_{k=0}^{L} \varepsilon_{t+k}^{T} S_{t+k}^{-1} \varepsilon_{t+k} - \left(\varepsilon_{t+k} - \varphi_{t+k}^{T}\hat{\nu}_t\right)^{T} S_{t+k}^{-1} \left(\varepsilon_{t+k} - \varphi_{t+k}^{T}\hat{\nu}_t\right).$$

By using the equivalent statistic

$$\tilde{T}_t = \left(\sum_{k=0}^{L} \varepsilon_{t+k}^{T} S_{t+k}^{-1} \varphi_{t+k}^{T}\right) \hat{\nu}_t \quad (20)$$

a straightforward expression of the threshold is obtained. Indeed, the test statistic $\tilde{T}_t$ is Gaussian, hence

$$\tilde{h}_t = \sigma_T \phi^{-1}(1-\alpha) \quad (21)$$

where

- $\phi(x) = \int_{-\infty}^{x} (1/\sqrt{2\pi}) \exp(-(x^2/2))\, \mathrm{d}x$;
- $\sigma_T = \sqrt{\hat{\nu}_t^{T} (\sum_{k=0}^{L} \varphi_{t+k} S_{t+k}^{-1} \varphi_{t+k}^{T}) \hat{\nu}_t}$ is the standard deviation of $\tilde{T}_t$.

By comparing the approximated test statistic $\tilde{T}_t$ and the corresponding threshold $\tilde{h}_t$, the algorithm can state whether GPS pseudoranges are incurring a mean jump or not.

Resampling Procedure: A straightforward use of the statistic test would consist of directly discarding particles that indicate the wrong hypothesis. However, the convergence properties of the PF would not be guaranteed anymore. As an alternative, the result of the hypothesis test can be used to design a more efficient proposal distribution for the resampling step. The possible flexibility in choosing the resampling weights has already been emphasized for instance in [26]. Instead of resampling according to the filtering weights, auxiliary weights may be used that reflect certain "future trend." Such approaches have already been extensively studied as an improvement of the PF simulation step (see [27] and [28]). The new set of generated particles is assigned corrected weights according to the importance sampling rule, thereby ensuring that the random samples still form an approximation of the target distribution $P[\lambda_t|\boldsymbol{Y}_{1:t}]$. If a mean jump is detected, the following rule can be applied to compute the auxiliary weights:

- $\alpha_t^{(i)} = (\tilde{\omega}_t^{(i)})^{\beta}$ for the particles which disagree with the result of the test;
- $\alpha_t^{(i)} = \tilde{\omega}_t^{(i)}$, otherwise;

where the coefficient of penalization β ($\beta > 1$) can be interpreted as the chance that the associated particles survive after a few iterations. The modified resampling operates by randomly selecting a particle $\lambda_t^{(i)}$ from $\{\lambda_t^{(k)}\}_{k=1:N}$ with probability $\alpha_t^{(k)}$. The particle is then assigned the filtering weight $\omega_t^{(i)} = \omega_t^{(k^i)}/\alpha_t^{(k^i)}$ when sample $\lambda_t^{(k^i)}$ is selected. By favoring the particles which are the more likely to live on, this technique ensures that efficient proposals are used to simulate the particles at the next time steps. It can be interpreted as an attempt to reduce the variability of the PF importance weights. The PF behavior is therefore improved for a moderate number of particles. The final algorithm allowing us to estimate the state vector $\boldsymbol{X}_t$ and the indicator sequence $\lambda_{0:t}$ is summarized in Table I.

TABLE I
FIXED-LAG RBPF FOR JOINT DETECTION/ESTIMATION OF MULTIPATH DEGRADATIONS

- Initialization: $\begin{cases} \boldsymbol{X}_0^{(i)} \sim p(\boldsymbol{X}_0), \\ \omega_t^{(i)} = 1/N, \end{cases}$ for $i = 1, \ldots, N$.
- For $t = 1, \ldots, T$:
  - Simulation step, for $i = 1, \ldots, N$:
    - ▶ run L iterations of n_Λ parallel EKFs corresponding to hypotheses $\left(\boldsymbol{\Lambda}_0^{t+L}\right)^{(i,j)}$ $(j = 1, \ldots, n_\Lambda)$.
    - ▶ $\lambda_t^{(i)} \sim P\left[\lambda_t | \lambda_{0:t-1}^{(i)}, \lambda_{t+1:t+L} = \mathbf{0}, \boldsymbol{Y}_{1:t+L}\right]$.
  - Weighting: compute $\begin{cases} \text{filtering weights } \omega_t^{(i)} \text{ according to (8),} \\ \text{smoothing weights } \tilde{\omega}_t^{(i)} \text{ according to (9).} \end{cases}$
  - Mean jump test:
    - ▶ compute $\tilde{T}_t$ and $\tilde{h}_t$ according to (21) and (20),
    - ▶ if $\tilde{T}_t \geq \tilde{h}_t$, a mean jump is detected, set $\begin{cases} \alpha_t^{(i)} = \left(\omega_t^{(i)}\right)^{\beta} \text{ if } \lambda_t^{(i)} = \mathbf{0}, \\ \alpha_t^{(i)} = \omega_t^{(i)} \text{ otherwise,} \end{cases}$ for $i = 1, \ldots, N$.
    - ▶ if $\tilde{T}_t \leq \tilde{h}_t$, set $\alpha_t^{(i)} = \omega_t^{(i)}$for $i = 1, \ldots, N$.
    - ▶ Normalization of the auxiliary weights $\alpha_t^{(i)}$, for $i = 1, \ldots, N$.
  - Estimation: compute $\widehat{\boldsymbol{X}}_t$ and P_t^c as in (10) and (11).
  - Resampling, for $i = 1, \ldots, N$: $\begin{cases} \lambda_t^{(i)} = \lambda_t^{(j^i)} \text{ with } j^i \sim \sum_{j=1}^{N} \alpha_t^{(j)} \delta_j, \\ \omega_t^{(i)} = \omega_t^{(j^i)}/\alpha_t^{(j^i)}. \end{cases}$

TABLE II
SIMULATION PARAMETERS

Process noise (velocity)	$\sigma_a = 1\ \mathrm{m/s}^{-2}$
Process noise (bias)	$\sigma_m = 0.1\ \mathrm{m}$
GPS measurement noise	$\sigma\ = 10\ \mathrm{m}$

V. SIMULATION RESULTS

Several simulations have been conducted to study the performance of the proposed algorithm. The state space model has been simulated with the parameters given in Table II. These parameters correspond to a nearly straight uniform motion. The fault-free GPS measurements have been computed from almanac files listing all useful information about GPS satellite orbital motion. Different multipath scenarios have been tested by randomly adding biases of various amplitudes and durations to these pseudoranges. The joint detection/estimation PF has been compared to existing methods (GLR, multiple model algorithm) through different criteria

- **detection capability**: the ability to detect multipath biases of small amplitudes is investigated together with the chance of missed detections by studying the estimated change probability $\hat{P}_t^c$;
- **estimation accuracy**: for both the navigation states and multipath biases, $M = 50$ Monte Carlo runs are averaged to compute the root mean square errors (rmses) defined by $\sqrt{M^{-1}\sum_{k=1}^{M}(\hat{\boldsymbol{X}}_t^{(k)} - \boldsymbol{X}_t)^2}$, where $\hat{\boldsymbol{X}}_t^{(k)}$ is the kth run estimate.

The multiple model (MM) algorithm proceeds by cutting off the less probable branches of the growing tree of possible hypotheses. To allow a fair comparison, the same lag and the same number of particles $N = 1024$ are used for the MM algorithm and the fixed-lag Rao-Blackwellized particle filter (FL-RBPF). The lag L, equal to 5, also determines the size of the observation window for the GLR. Finally, the penalizing factor β is set to 2.

A. Bias Estimation

The accuracy achieved by the three algorithms for multipath biases estimation is depicted on Figs. 1 and 2 for one of the simulated scenarios. Two of the GPS pseudoranges, corresponding to the satellites with the lowest elevation angles, experience simultaneous multipath perturbations. Fig. 1 shows the estimated biases versus time. The corresponding estimation errors are plotted on Fig. 2. The GLR fails to track the biases probably because no *a priori* information about the jump amplitudes is taken into account. The two other algorithms provide better results. However, the PF shows a smaller response time after a mean value jump. In addition, the PF bias estimates visually seem more stable. Note that the tracking performance of both approaches are similar when the amplitudes of the mean jumps are high enough.

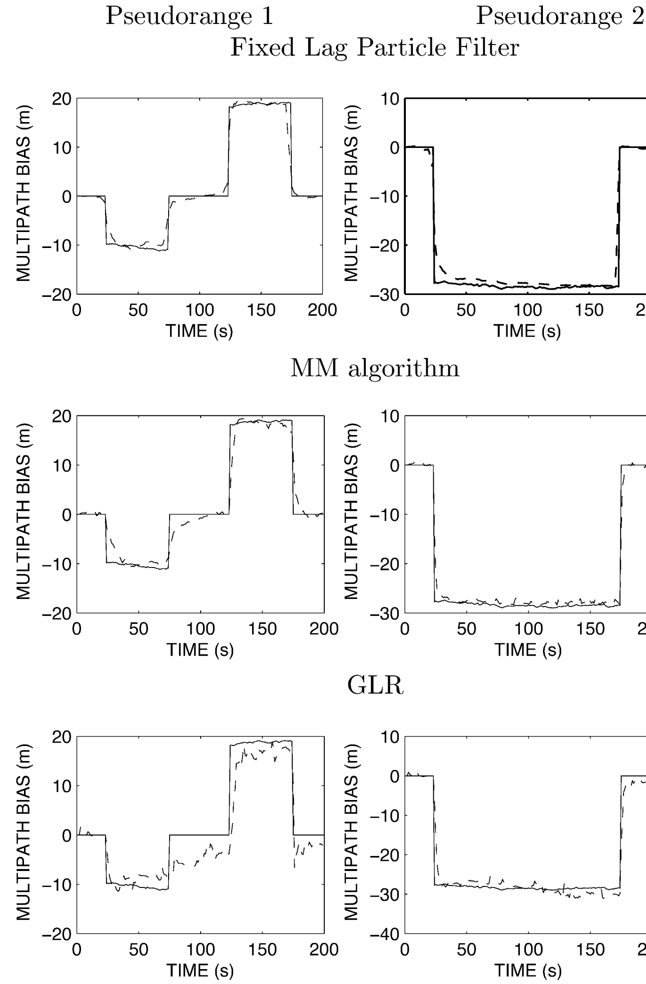

Fig. 1. Estimation of multipath biases (50 Monte Carlo runs). The actual bias is shown in solid line while the mean estimated biases are plotted as dotted lines.

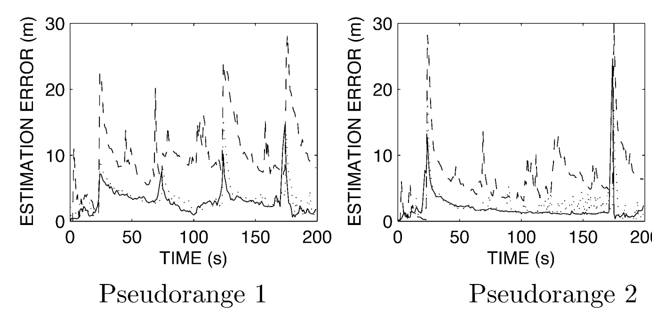

Fig. 2. Multipath bias estimation errors (50 Monte Carlo runs). RBPF: Solid line; GLR: dashed line; MM algorithm: dotted line.

B. Detection Capability

Posterior Change Probabilities: Fig. 3 shows the *posterior* change probabilities for the MM algorithm and the particle filter for different values of the lag L. The influence of this parameter is clearly emphasized. In the absence of lag, it is almost impossible to locate mean jumps of small amplitudes. On the contrary, the change probability peaks clearly coincide with the change instants with a lag $L = 5$. Note that the peaks are more pronounced for the fixed lag PF than for the MM algorithm due to a more efficient strategy to select relevant model hypotheses.

Detection Performance: Mean jumps of different amplitudes have been introduced on the GPS measurements to investigate the robustness of the RBPF and the MM technique. For each scenario, the mean detection delay $\bar{\tau}$ and its standard deviation σ_τ have been computed by averaging 50 realizations. The detection delay is defined as the absolute estimation error of the change

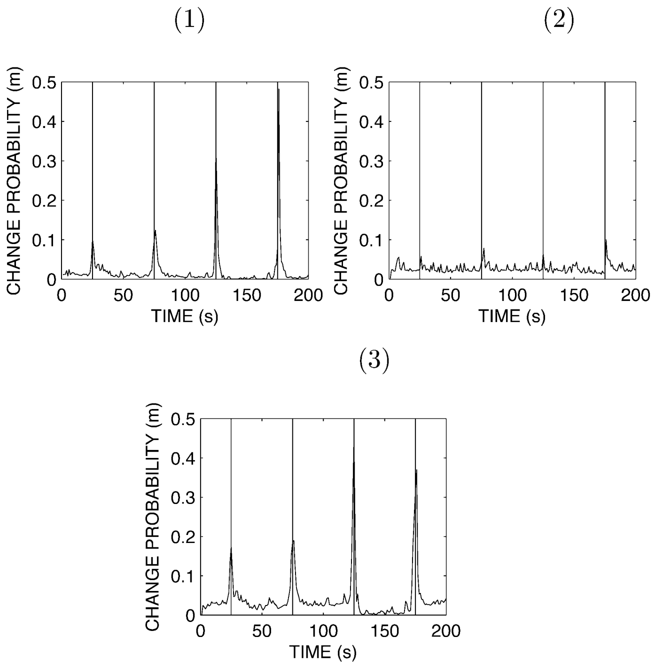

Fig. 3. *Posterior* change probabilities (50 Monte Carlo runs). (1) MM algorithm. (2) Fixed Lag PF, $\mathrm{L} = 1$. (3) Fixed Lag PF, $\mathrm{L} = 5$.

TABLE III
DETECTION PERFORMANCE FOR MEAN JUMPS OF DIFFERENT AMPLITUDES

Mean jump amplitude (meters)	RBPF			MM algorithm		
	$\bar{\tau}$	σ_τ	P_{md}	$\bar{\tau}$	σ_τ	P_{md}
3	0.9	4.3	0.57	1.5	4.64	0.67
5	0.6	2.09	0.5	1.2	2.06	0.65
10	0.7	2.16	0.25	0.9	2.01	0.35
15	0.44	1.64	0.03	0.7	1.79	0.03
18	−0.23	1.55	0.01	−0.29	2.47	0.01
28	0.01	0.67	0	−0.14	0.79	0
35	0.01	0.38	0	0.06	0.62	0

instants and a detection occurs whenever the estimated change probability exceeds a given threshold. The obtained values are reported in Table III as well as the missed detection probability P_{md}. The results confirm that biases which are embedded in the measurement noise (amplitude inferior to 10 meters) are difficult to detect, leading to high values of P_{md}. In this case, nearly half of the emulated mean jumps are not properly located. A closer analysis of Table III reveals that the RBPF achieves shorter detection delays and yields smaller values of the P_{md}. It is worth noticing that the difference between both approaches tends to become less marked as the amplitudes of multipath errors increases.

Multiple Multipath Error Detection: Finally, it is important to ensure that the algorithms can handle several mean jumps occurring at the same time. The simulation presented here considers two pseudoranges degraded simultaneously. The estimated numbers of multipath components for 50 Monte Carlo runs are presented in Fig. 4. The simulation results show that RPBF provides more reliable results than the MM solution.

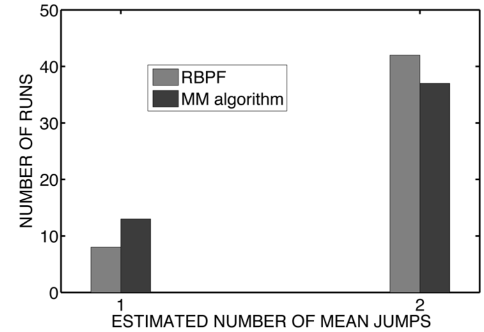

Fig. 4. Number of estimated simultaneous mean jumps for 50 Monte Carlo runs.

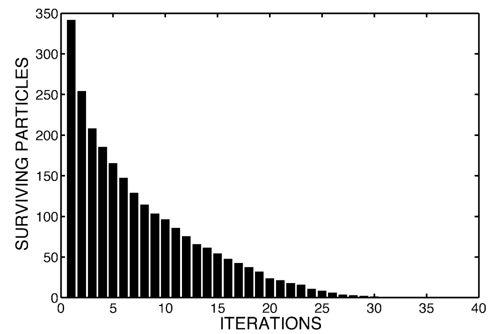

Fig. 5. Mean number of particles refuting the result of the hypothesis test.

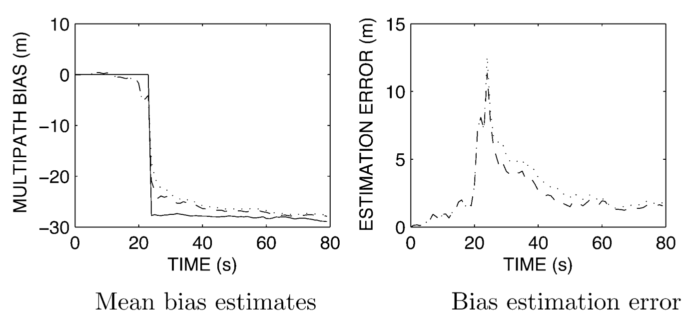

Fig. 6. Comparison of the decision-aided resampling and a classical resampling procedure (50 Monte Carlo runs). Solid line: Actual bias; dashed line: aided resampling; dotted line: classical resampling.

C. Gain of Aided-Resampling

It is important to make sure that the particles whose weights are penalized through decision-aided resampling were likely to disappear a few iterations later. Fig. 5 shows the average number of particles (out of $N = 1024$) which do not detect a mean jump and survive for the next iterations. The results have been obtained for biases of different amplitudes by averaging 50 Monte Carlo runs. All the particles disagreeing with the result of the hypothesis test are naturally discarded after a maximum of 30 iterations. The decision-aided resampling proposed in this paper is an attempt to speed up this removal process, thereby improving multipath bias tracking.

The impact of the decision-aided resampling on multipath bias estimation is then investigated. The bias estimates and the corresponding estimation errors obtained with the PF in presence or absence of decision-aided are shown on Fig. 6. The decision-aided resampling yields on average tighter estimates, especially after apparition of a multipath bias.

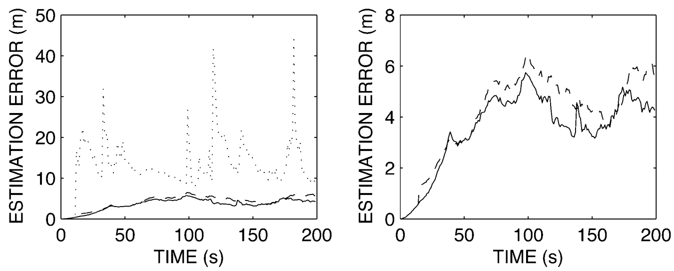

Fig. 7. Position estimation error (50 Monte Carlo runs). Solid line: RBPF; dashed line: MM algorithm; dotted line: GLR.

D. Position Estimation

Fig. 7 shows the position estimation errors for the three algorithms so as to evaluate the impact of multipath event detection on the navigation solution. Unsurprisingly, the GLR performs poorly due to the inaccuracy of the bias estimates. The advantage of the PF approach over the MM algorithm for change detection has a slight impact on the position estimates, yielding a smallest estimation error. However, it is important to note that reliable multipath event detection is nonetheless crucial to inform the user on the trust he can place in the computed navigation solution.

Before concluding, it is worth giving a rough idea of the computational complexity of the different algorithms. All simulations have been coded using MATLAB and performed on a 512–MHz Athlon. One run of 200 iterations requires on average 1 min for the GLR, 15 min for the MM solution and 25 min for the proposed PF algorithm.

VI. Conclusion

This paper studied a particle filter algorithm to mitigate multipath effects in GPS navigation. An original approach was proposed whereby the navigation algorithm jointly tackles the detection and estimation of multipath errors while inferring the vehicle dynamics. Multipath events were considered as abrupt changes affecting the navigation state space model. A particle filter approach was adopted due to its flexibility to explore and select proper model hypotheses. The proposed algorithm included an approximate fixed lag delay sampling, smoothing estimates and a decision aided resampling. The three steps were shown to improve the detection of multipath events as well as the estimation of the induced biases and the navigation states. The method compared favorably with the algorithms conventionally used for abrupt change detection, i.e., the GLR and MM approaches.

It is important to note that this method is independent of the GPS receiver technology so that it can be widely applied. Moreover, another advantage of the PF strategy is that it can be easily extended to detect and estimate other perturbations, such as variance jumps due to jamming. The extension of the proposed algorithm to detect and estimate interferences affecting GPS measurements has been introduced in [29] and is currently under investigation. This method could also be applied to multiple object tracking by considering a more elaborate multipath model. In particular, targets which are close to each other are likely to be affected simultaneously by a multipath mean jump.

Appendix
PF Approximation of the Measurement Predictive Distributions

Section IV-B–3 argues that the PF approximates the measurement predictive distributions by mixtures of Gaussian distributions. This assertion is confirmed hereafter and the corresponding importance weights are computed. At time instant t, the predictive pdfs under hypothesis $H_{0,t}$ can be expressed as

$$\begin{aligned} p(\boldsymbol{Y}_{t+k}|\boldsymbol{Y}_{1:t+k-1}, H_{0,t}) &= \sum_{\boldsymbol{\lambda}_{0:t-1}} p(\boldsymbol{Y}_{t+k}|\boldsymbol{Y}_{1:t+k-1}, \boldsymbol{\lambda}_{0:t-1}, H_{0,t}) \\ &\quad \times p(\boldsymbol{\lambda}_{0:t-1}|\boldsymbol{Y}_{1:t+k-1}, H_{0,t}) \end{aligned}$$

for $k = 0, \ldots, L$. PF estimates of the conditional distributions of the indicator vector are available

$$p(\boldsymbol{\lambda}_{0:t-1}|\boldsymbol{Y}_{1:t+k-1}, H_{0,t}) \simeq \sum_{i=1}^{N} \beta_{t+k}^{(i)} \delta\left(\boldsymbol{\lambda}_{0:t-1} - \boldsymbol{\lambda}_{0:t-1}^{(i)}\right).$$

with $\beta_t^{(i)} \propto \omega_{t-1}^{(i)}$ and

$$\beta_{t+k}^{(i)} \propto \omega_{t-1}^{(i)} \prod_{l=1}^{k} p\left(\boldsymbol{Y}_{t+l-1}|\boldsymbol{Y}_{1:t+l-2}, \boldsymbol{\lambda}_{0:t-1}^{(i)}, H_{0,t}\right)$$

for $k > 0$. It follows:

$$p(\boldsymbol{Y}_{t+k}|\boldsymbol{Y}_{1:t+k-1}, H_{0,t}) \simeq \sum_{i=1}^{N} \beta_{t+k}^{(i)} p(\boldsymbol{Y}_{t+k}|\boldsymbol{Y}_{1:t+k-1}, \boldsymbol{\lambda}_{0:t-1}, H_{0,t}).$$

Acknowledgment

The authors would like to thank A. Monin for interesting discussions regarding multipath modeling and M. Davy and A. Doucet for very helpful comments regarding the proposed particle filtering algorithm.

References

[1] R. Kalman, “A new approach to linear filtering and prediction problems,” *Trans. ASME*, pp. 35–45, 1960.
[2] B. Anderson and J. Moore, *Optimal Filtering*. Englewood Cliffs, NJ: Prentice-Hall, 1979.
[3] A. Doucet, de Freitas, and N. Gordon, *Sequential Monte Carlo Methods in Practice*. New York: Springer, 2001.
[4] P. Djuric, J. Kotecha, J. Zhang, Y. Huang, T. Ghirmai, M. Bugallo, and J. Miguez, “Particle filtering,” *IEEE Signal Process. Mag.*, vol. 20, no. 5, pp. 19–38, 2003.
[5] F. Gustafsson, *Adaptive Filtering and Change Detection*. New York: Wiley, 2000.
[6] M. Basseville and I. Nikiforov, *Detection of Abrupt Changes: Theory and Application*. Englewood Cliffs, NJ: Prenctice-Hall, 1993.
[7] Y. Bar-Shalom, X. Rong Li, and T. Kirubarajan, *Estimation with Applications to Tracking and Navigation*. New York: Wiley, 2001.
[8] A. Doucet, S. Godsill, and C. Andrieu, “On sequential Monte Carlo sampling methods for Bayesian filtering,” *Statist. Comp.*, vol. 10, pp. 197–208, 2000.
[9] A. Doucet, N. Gordon, and V. Krishnamurthy, “Particle filters for state estimation of jump Markov linear systems,” *IEEE Trans. Signal Process.*, vol. 49, no. 3, pp. 613–624, Mar. 2001.

[10] T. Clapp and S. Godsill, "Fixed-lag smoothing using sequential importance sampling.," in *Bayesian Statistics VI*, J. Bernardo, J. Berger, A. Dawid, and A. Smith, Eds. New York: Oxford Univ. Press, 1999, pp. 743–752.

[11] X. Wang, R. Chen, and D. Guo, "Delayed pilot sampling for mixture Kalman filter with application in fading channels," *IEEE Trans. Signal Process.*, vol. 50, no. 2, pp. 241–253, Feb. 2002.

[12] E. Kaplan, *Understanding GPS, Principles and Applications*. Boston, MA: Artech House, 1996.

[13] J. Soubielle, I. Fijalkow, P. Duvant, and A. Bibaut, "GPS positioning in a multipath environment," *IEEE Trans. Signal Process.*, vol. 50, no. 1, pp. 141–150, Jan. 2002.

[14] L. Garin, F. Van Diggelen, and J. Rousseau, "Strobe and edge correlator multipath rejection for code and carrier," in *Proc. ION GPS-96*, Kansas City, MO, Sep. 17–20, 1996.

[15] L. Garin and J. Rousseau, "Enhanced strobe correlator multipath rejection for code and carrier," in *Proc. ION GPS-97*, Kansas City, MO, Sep. 16–19, 1997.

[16] R. A. Iltis, "A sequential Monte Carlo filter for joint linear/nonlinear state estimation with application to DS-CDMA," *IEEE Trans. Signal Process.*, vol. 51, no. 2, pp. 417–426, Feb. 2003.

[17] G. I. Jee, H. S. Kim, and C. G. Park, "A GPS C/A code tracking loop based on extended Kalman with multipath mitigation," in *Proc. ION GPS-02*, Portland, OR, Sep. 24–27, 2002, pp. 446–451.

[18] M. Najar, J. Huerta, J. Vidal, and A. Castro, "Mobile location with bias tracking in non-line-of-sight," *Proc. IEEE Int. Conf. Acoustics, Speech, Signal Processing (ICASSP)*, vol. 3, pp. 956–961, May 17–21, 2004.

[19] J. Farrell and M. Barth, *The Global Positioning System and Inertial Navigation*. New-York: McGraw-Hill, 1999.

[20] A. Giremus, A. Doucet, J. Tourneret, and A. Escher, "Non linear filtering approaches for GPS/INS integration," in *EUSIPCO-04*, F. Hlawatsch, G. Matz, M. Rupp, and B. Wistawel, Eds., Vienna, Austria, Sep. 2004, pp. 873–876, Elsevier.

[21] R. Chen and S. Liu, "Mixture Kalman filters," *J. Roy. Stat. Soc.*, vol. 62, no. 3, pp. 493–508, 2000.

[22] P. Nordlund, "Recursive state estimation of nonlinear systems with applications to integrated navigation," Dep. Elect. Eng. Linkping Univ., Tech. Rep. SE-58183, Nov. 2001.

[23] C. Andrieu, M. Davy, and A. Doucet, "Efficient particle filtering for Jump Markov Systems. Application to time-varying autoregressions," *IEEE Trans. Signal Process.*, vol. 51, no. 7, pp. 1762–1770, Jul. 2003.

[24] A. Doucet and C. Andrieu, "Particle filtering for partially observed Gaussian state space models," *J. Roy. Stat. Soc.*, vol. 64, no. 4, pp. 827–836, 2002.

[25] A. Willsky and H. Jones, "A generalized likelihood ratio approach to the detection and estimation of jumps in linear systems," *IEEE Trans. Autom. Control*, vol. 21, pp. 108–112, 1976.

[26] A. J. Liu, R. Chen, and T. Logvinenko, "A theoretical framework for sequential importance sampling with resampling," in *Sequential Monte Carlo Methods in Practice*, A. Doucet, N. de Freitas, and N. Gordon, Eds. New York: Springer-Verlag, 2001, pp. 225–246.

[27] S. Godsill and T. Clapp, "Improvement strategies for Monte Carlo particle filters," in *Sequential Monte Carlo Methods in Practice*, A. Doucet, N. de Freitas, and N. Gordon, Eds. New York: Springer-Verlag, 2001, pp. 225–246.

[28] M. K. Pitt and N. Shepard, "Auxiliary variable based particle filter," in *Sequential Monte Carlo Methods in Practice*, A. Doucet, N. de Freitas, and N. Gordon, Eds. New York: Springer-Verlag, 2001, pp. 225–246.

[29] A. Giremus, J. Tourneret, and A. Doucet, "A particle filter to mitigate jamming for GPS navigation," in *Proc. Stat. Signal Process. (SSP)*, Bordeaux, France, Jul. 2005.

Audrey Giremus received the engineer degree in 2002, and the Ph.D. degree in signal processing, both from Ecole Nationale Supèrieure de l'Aéronautique et de l'Espace (ENSAE), Toulouse, France, in December 2005.

Her research interests include detection, estimation, and statistical signal processing. She is currently working on particle filtering techniques for application to radio navigation and inertial positioning.

Jean-Yves Tourneret received the ingénieur degree in electrical engineering from Ecole Nationale Supérieure d'Electronique, d'Electrotechnique, d'Informatique et d'Hydraulique, Toulouse (ENSEEIHT), France. He received the Ph.D. degree from the National Polytechnic Institute, Toulouse, in 1992.

He is currently a professor with the University of Toulouse, France, (ENSEEIHT). He is also a member of the IRIT Laboratory (UMR 5505 of the CNRS), where his research activity is centered around estimation, detection and classification of non-Gaussian and nonstationnary processes.

Dr. Tourneret was the program chair of the European Conference on Signal Processing (EUSIPCO), Toulouse, in 2002. He is also member of the ICASSP'06 organizing committee. He has been a member of different technical committees including the Signal Processing Theory and Methods (SPTM) committee of the IEEE Signal Processing Society.

Vincent Calmettes received the Ph.D. degree in signal processing from SUPAERO (ENSAE), Toulouse, France.

He is the Head of the Laboratory of Electronics and Physics, SUPAERO, Toulouse, France. His research interests include the development of solutions based on DSP processors and programmable logic devices or ASICs for applications in digital communications and signal processing. He is also currently working on new Galileo signal processing.